INL/JOU-20-59780-Revision-0

RELAP5-3D modelling of the HTTR-GT/H2 secondary system and turbomachinery

April 2022

Nolan A Anderson, Paul W Humrickhouse, C. Rabiti, H. Sato, X.L. Yan

Changing the World's Energy Future

INL is a U.S. Department of Energy National Laboratory operated by Battelle Energy Alliance, LLC

DISCLAIMER

This information was prepared as an account of work sponsored by an agency of the U.S. Government. Neither the U.S. Government nor any agency thereof, nor any of their employees, makes any warranty, expressed or implied, or assumes any legal liability or responsibility for the accuracy, completeness, or usefulness, of any information, apparatus, product, or process disclosed, or represents that its use would not infringe privately owned rights. References herein to any specific commercial product, process, or service by trade name, trade mark, manufacturer, or otherwise, does not necessarily constitute or imply its endorsement, recommendation, or favoring by the U.S. Government or any agency thereof. The views and opinions of authors expressed herein do not necessarily state or reflect those of the U.S. Government or any agency thereof.

INL/JOU-20-59780-Revision-0

RELAP5-3D modelling of the HTTR-GT/H2 secondary system and turbomachinery

Nolan A Anderson, Paul W Humrickhouse, C. Rabiti, H. Sato, X.L. Yan

April 2022

Idaho National Laboratory
Idaho Falls, Idaho 83415

http://www.inl.gov

Prepared for the
U.S. Department of Energy
Under DOE Idaho Operations Office
Contract DE-AC07-05ID14517

RELAP5-3D Modelling of the HTTR-GT/H_2 Secondary System and Turbomachinery

N. A. Anderson [a,1], P. W. Humrickhouse [a], C. Rabiti [a], H. Sato [b], and X. L. Yan [b]
[a] *Idaho National Laboratory, 1955 N. Fremont Ave., Idaho Falls, ID 83415*
[b] *Japan Atomic Energy Agency, 4002 Narita-cho, Oarai-Machi, Ibaraki, Japan*

Abstract

High Temperature Gas-cooled Reactors (HTGRs) can be used for the cogeneration of electricity and hydrogen. The JAEA-operated High-Temperature engineering Test Reactor (HTTR-GT/H_2) is exploring using the reactor for electricity and hydrogen production. A RELAP5-3D model of the HTTR-GT/H_2 secondary system has been developed using design information. The various components and heat exchangers in the secondary system were investigated, modified, and improved where applicable. With these changes made, the model was run, and the results were compared to the design conditions. The results for the sole-power generation mode were shown to fit the design conditions very well. The largest temperature difference was on the order of 7 K, and the largest pressure difference was on the order of 0.05 MPa. The results for the hydrogen cogeneration mode did not fit the design conditions as well as the other case. The largest temperature difference was about 39 K and the largest pressure difference was about 0.27 MPa at the compressor outlet. The larger differences for the hydrogen cogeneration mode are attributed to the various complex components and the flow being split in the secondary loop.

A transient reduction in heat removal capability of the secondary system was investigated. Reactor temperatures were predicted to rise as a result. The core reactivity response due to this increase in temperature is investigated and is expected to add negative reactivity to the reactor.

1.1 Introduction

"A High Temperature Gas-cooled Reactor (HTGR) is useful for cogeneration of electricity and hydrogen, as well as for other process-heat applications, related to the chemical, oil, and iron industries. It is able to produce hydrogen from water by using thermochemical, electrochemical, or hybrid processes with reduced emission of CO_2 gases" (Pioro and Duffey, 2019). The HTGR offers enhanced safety features and high temperature capabilities (IAEA, 2010). The High Temperature engineering Test Reactor (HTTR) is a HTGR test reactor built in Japan and operated by the Japan Atomic Energy Agency (JAEA) (HTTR Website, 2020). The outlet temperature (950°C) of the HTTR is sufficiently high that the process heat could be used for hydrogen production (Fujikawa, S., Hayashi, H., et al., 2004). JAEA is exploring utilizing the HTTR to cogenerate both electricity and hydrogen. The HTTR would be able to be operated in two modes, Sole Power Generation (SPG) and Hydrogen Co-Generation (HCG). In the SPG mode the reactor is used to generate electricity only using the Brayton cycle. In the HCG mode the reactor heat is split so that a portion is used to generate electricity and the remainder is transferred as process heat to a tertiary

[1] Corresponding author at: Idaho National Laboratory, 1955 N. Fremont Ave., Idaho Falls, ID 83415
Email: Nolan.Anderson@inl.gov

system for the Sulfur-Iodine process which is used to produce hydrogen. The design of the secondary system of the HTTR is such that the reactor heat can be used to generate electricity via Gas Turbine (GT) and/or hydrogen (H_2) Thus the reactor system is called the HTTR-GT/H_2.

The RELAP5-3D software was originally developed to model reactor transient behavior for light-water reactor systems (The RELAP5-3D© Code Development Team, 2018). Coding developments have made it possible to model both nuclear and non-nuclear systems and a variety of working fluids and system behavior. In particular, the software has been used to model high temperature gas cooled systems (Sterbentz and Bayless, 2015 and Davis, Siefken, et al., 2005).

A secondary system model of the HTTR-GT/H_2 was modeled previously with RELAP5-3D (Humrickhouse, 2018). Some information was not available previously which required the use of temporary or incomplete components to model portions of the system. In addition, it was reported that the turbine component could not properly model the pressure drop because it did not have the capability of modeling the form losses correctly.

JAEA provided additional component detail which allowed for model improvement (Imai, Sato, et al., 2017). The modeling changes and improvements that were made to the existing model are described in this document.

The description of the model given in (Humrickhouse, 2018) is reiterated here, and the improvements to the model are also described.

A transient analysis was also performed by reducing the mass flow rate in the secondary system and observing the response of the primary system. The reduced cooling capability of the secondary system results in an increased primary system temperature. The potential reactivity effects of this temperature increase are evaluated.

2.1 Secondary System Modeling

The secondary system of the HTTR-GT/H_2 is depicted in Figure 1 (Humrickhouse, 2018). The two different system arrangements SPG and HCG are shown in the figure, where the operation mode can be switched from SPG mode (blue) to HCG mode (green) by operator action.

In SPG mode 10 MW of heat is removed from the primary system by the helium gas flowing at 9.85 kg/s and exits the intermediate heat exchanger (IHX) at 570°C. The helium gas travels to the turbines and upon exiting the turbines it flows into an integrated heat exchanger consisting of an offset strip plate/fin recuperator and helical coil precooler. After travelling through the compressors, it passes through the high-pressure side of the recuperator, and is then cooled to the appropriate IHX inlet temperature (374°C) by Cooler A.

In HCG mode the flow rate through the IHX is greatly reduced to 2.57 kg/s to increase the outlet helium temperature to 900°C. This high-temperature helium transfers heat via a 2nd IHX to a tertiary helium loop and hydrogen plant before merging with a 6.58 kg/s recirculating helium flow and entering the turbines. The combined helium flow of 9.15 kg/s travels through the turbomachinery and integrated heat exchanger. Upon exiting the high-pressure side of the recuperator, 6.58 kg/s is sent back to the

turbines and the remaining 2.57 kg/s is cooled to 150°C and sent to Cooler B (which differs from Cooler A because of a reduced flow rate and different heat transfer rate) before returning to the IHX.

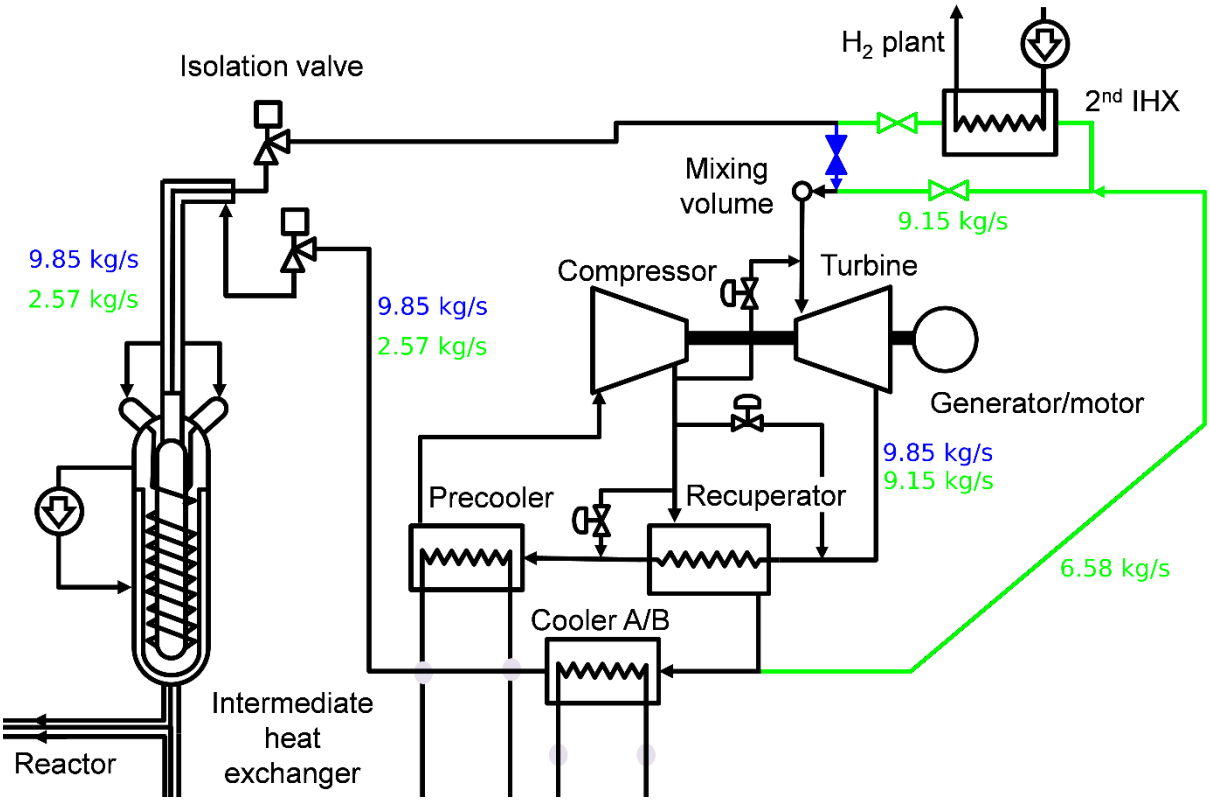

Figure 1. HTTR-GT/H_2 secondary system layout. Where they differ, the helium flow rates and paths in SPG mode are shown in blue, and for HCG mode in green.

The individual components of the secondary system were modeled independently before combining the entire secondary system loop as reported previously (Humrickhouse, 2018). The input model and individual components were created in a spreadsheet which ensured that any changes made to a component were propagated through the model. Some components were not modified as a part of this effort, where the current model was deemed sufficient, but are still described in this document.

Piping dimensions are obtained from a design database document (Imai, Sato, et al., 2017). A nodalization diagram of the HTTR secondary system is shown in Figure 2.

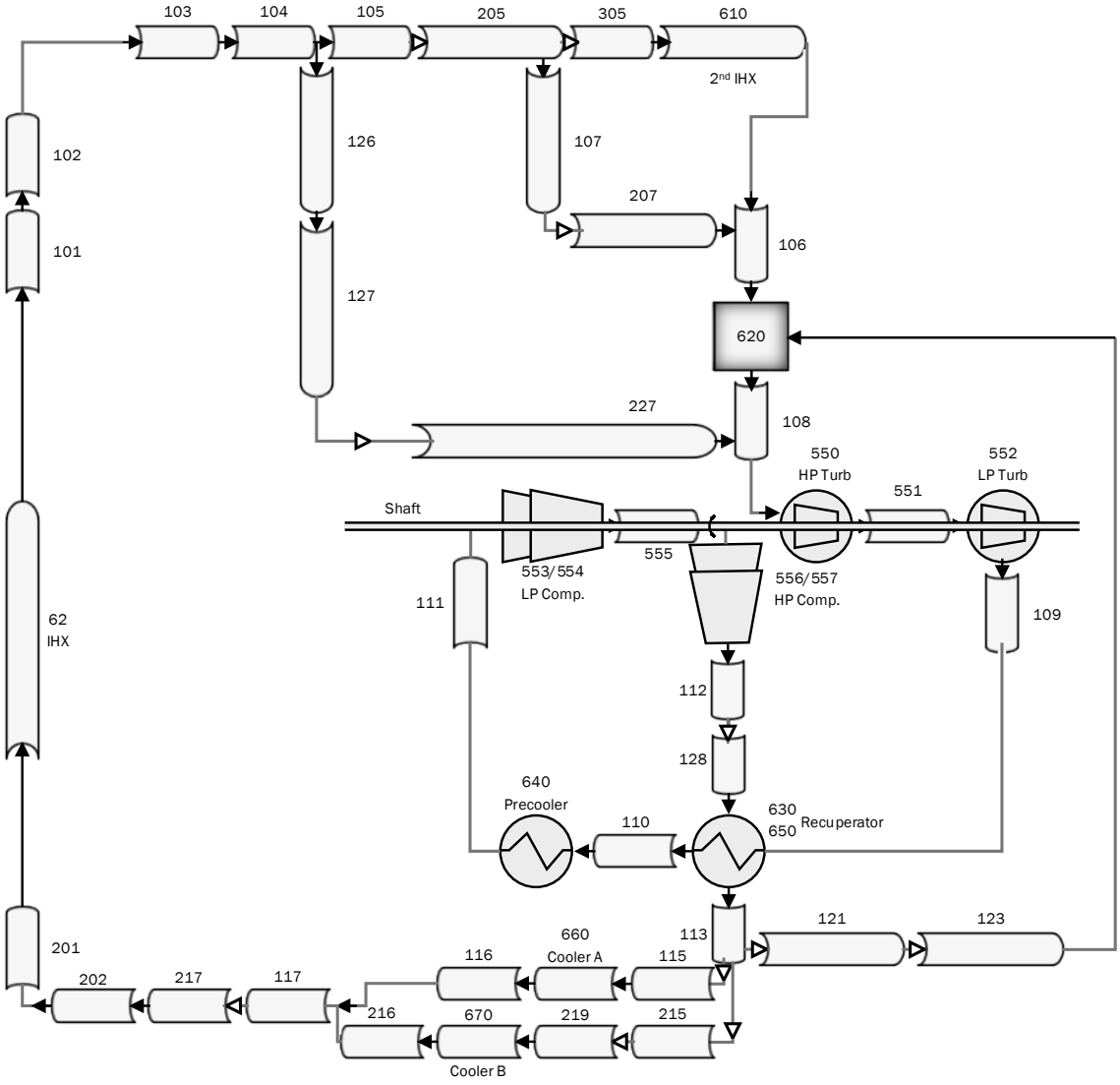

Figure 2. HTTR-GT/H_2 secondary system nodalization diagram.

2.1.1 Turbomachinery

The system turbomachinery consists of two single stage radial turbines and two two-stage centrifugal compressors. Both the high- and low-pressure turbines and compressors are geared down to a common shaft, a layout that reduces shaft vibration. Further details on the turbomachinery design are available in (Sato, Nomoto, et al., 2016, Yan, Sato, et al., 2016, and Tsukamoto, Oyama, et al., 2016).

2.1.1.1 Turbines

The high-pressure and low-pressure turbine components are used in series to generate electricity in the secondary system. Turbine performance data for the HTTR-GT/H_2 are shown in Figure 3. These give corrected flow rate $\dot{m}\sqrt{T}/P$ of each turbine and the efficiency (η) as a function of flow coefficient ϕ. The flow coefficient is defined as the ratio of the impeller tip speed to the speed of the working fluid. Note that the values on these figures are proprietary and are intentionally unclear.

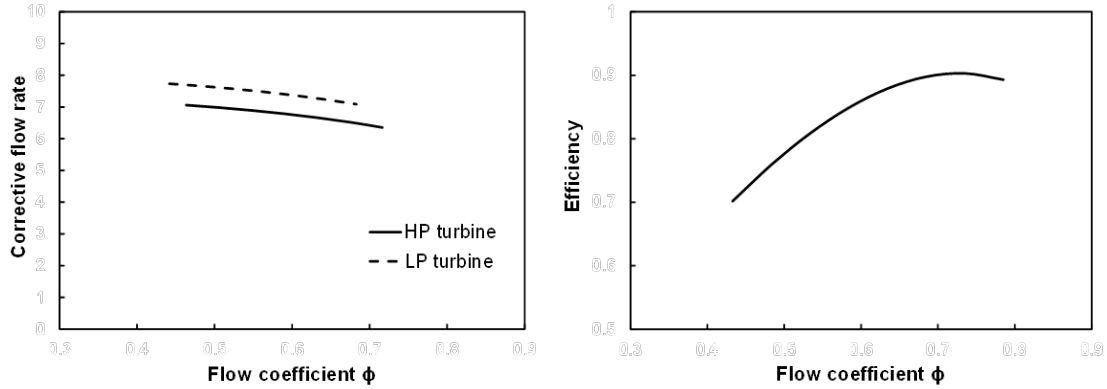

Figure 3. HTTR-GT/H_2 turbine performance data: corrective flow rate (a) and efficiency (b) (Imai, Sato, et al., 2017).

The turbines are modeled using the "Type 3" turbine model available in RELAP5-3D. This allows the specification of a variable efficiency.

$$\eta = \eta_R \left[\sum_{i=0}^{3} a_i \left(\frac{N}{N_R}\right)^i\right]\left[\sum_{j=0}^{3} b_j \left(\frac{\dot{W}}{\dot{W}_R}\right)^j\right] \cdot Mult \quad (1)$$

where N is the turbine speed, $\dot{W}$ is the turbine power, the subscript "R" refers to the rated conditions, and the multiplier "$Mult$" is set by a control variable. The constants a_i and b_j are specified by the user; a_0 and b_0 were set to 1.0 and the other constants were set to zero. Control variables were used to model the behavior of Figure 3 with variable $Mult$.

To do so, the relationship between the corrected flow rate and flow coefficient in Figure 3 (a) is approximated to be linear (which it nearly is in the range of flow coefficients provided). This relationship can then be inverted to give the flow coefficient as a function of corrected flow rate, $\phi\left(\dot{m}\sqrt{T}/P\right)$. A second (quadratic) relationship can be established between efficiency and flow coefficient from Figure 3 (b). This efficiency $\eta\left(\phi\left(\dot{m}\sqrt{T}/P\right)\right)$ is calculated with control variables from the flow conditions $\dot{m}$, T, and P using these two fits.

It was previously reported that there was no mechanism to calculate a variable form loss coefficient for the turbines (Humrickhouse, 2018). However, after additional investigation the RELAP5-3D turbine component was found to have the capability to model the form loss with a control variable.

The method used to calculate the form losses for the turbine components are described below.

The turbine form loss coefficient is defined by Equation 2 (Humrickhouse, 2018):

$$K = \frac{(1-\eta)(P_1 - P_2)}{0.5\rho v^2} \quad (2)$$

where η is the turbine efficiency, P_1 and P_2 are the pressure upstream and downstream of the turbine respectively, ρ is the helium density, and v is the helium velocity at the turbine inlet.

Using control variables, Equation 2 was initially used to calculate the form loss, but the RELAP5-3D code would minimize the pressure difference across the turbines to reduce the loss factor. This resulted in large flow rates through the system and an excessively small pressure drop across the turbine components that was not physically correct.

To obtain more reasonable results for the pressure drop across the turbine components, the pressure ratio relationship was used. The pressure ratio across the turbine component is defined as:

$$P_r = \frac{P_1}{P_2} \quad (3)$$

which can be written as $P_1 = P_r * P_2$.

Equation 3 is substituted into Equation 2 which yields

$$K = \frac{(1-\eta)(P_r - 1)P_2}{0.5\rho v^2} . \quad (4)$$

Control variables were then used to calculate the form loss based on Equation 4 across both the high- and low-pressure turbines. The pressure ratio across the turbines is defined in (Yan, Sato and Sumita, 2018) and is set to 1.13 for the high-pressure turbine and 1.15 for the low-pressure turbine. Pressure drop results compared favorably to design conditions when using Equation 4 to calculate the form loss coefficient.

2.1.1.2 Compressors

The compressor component is used to increase the gas pressure and transport the helium through the system. The compressor performance maps were provided by JAEA (Imai, Sato, et al., 2017), and curve fits to the data were generated. These compressor maps are displayed in Figure 4. These give the efficiency (η) and pressure coefficient (μ) of the compressors as a function of flow coefficient ϕ. Note that the values on these figures are proprietary and are intentionally unclear.

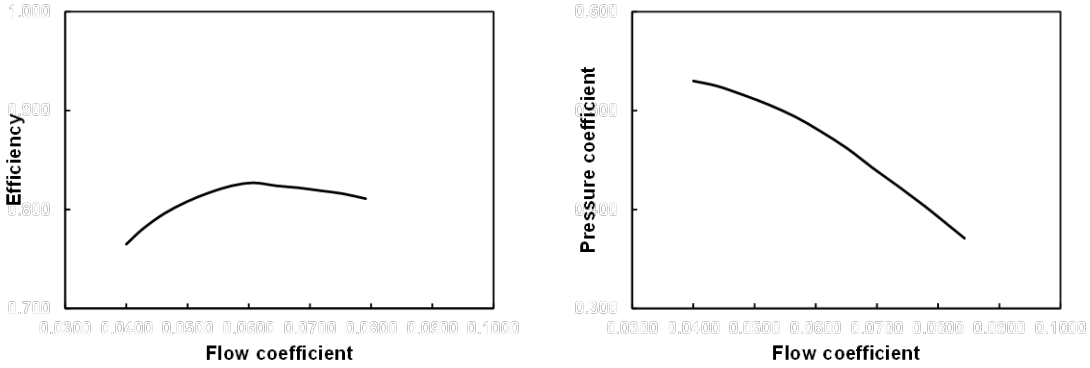

Figure 4. Compressor maps.

Empirical relationships were developed for the efficiency and pressure coefficient as a function of flow coefficient using the provided values from Figure 4.

The compressor flow coefficient is defined as

$$\varphi = \frac{Q}{\pi(D/2)^2 U} \tag{5}$$

where (Q) is the volumetric flow rate, (D) is the impeller outer diameter and (U) is the blade tip speed defined as:

$$U = \pi N D \tag{6}$$

where N is the compressor rotational speed.

When modeling the RELAP5-3D compressor component the performance maps are input as a series of tables that give the compressor efficiency (η) and pressure ratio (π_c) as functions of the relative corrected speed (α) and the relative corrected flow rate (v), which are defined below (Humrickhouse, 2018).

$$\alpha = \frac{\frac{N}{\sqrt{T}}}{\left(\frac{N}{\sqrt{T}}\right)_{rated}} \tag{7}$$

$$v = \frac{\frac{\dot{m}\sqrt{T}}{P}}{\left(\frac{\dot{m}\sqrt{T}}{P}\right)_{rated}} \tag{8}$$

Here T and P are the stagnation temperature and pressure at the compressor inlet. Using the ideal gas law and Equations 5 and 6, the flow coefficient can be written in terms of the corrected speed and flow,

$$\phi = \frac{4R_s}{\pi^2 D^3} \frac{\frac{\dot{m}\sqrt{T}}{P}}{\frac{N}{\sqrt{T}}} \tag{9}$$

where R_s is the specific gas constant. This can be solved for the relative corrected flow rate to give,

$$v = \frac{\pi^2 D^3 \phi \alpha \left(\frac{N}{\sqrt{T}}\right)_{rated}}{4R_s \left(\frac{\dot{m}\sqrt{T}}{P}\right)_{rated}} \tag{10}$$

The pressure ratio is given by (Imai, Sato, et al., 2017):

$$\pi_c = \left(1 + \frac{\mu \pi^2 D^2 \alpha^2}{Z R_s} \left(\frac{N}{\sqrt{T}}\right)^2_{rated} \left(\frac{\gamma - 1}{\gamma}\right)\right)^{\frac{\gamma}{\gamma - 1}} \tag{11}$$

where *Z* is the compressibility and γ is the specific heat ratio.

The RELAP5-3D input format is a series of tables, one for each relative corrected speed (α). Entries in each of these tables consist of three values— the relative corrected flow rate (υ), and the corresponding pressure ratio (π_c) and efficiency (η). For each table (or α), these values are determined for a range of flow coefficients using the empirical fits and Equations 10 and 11. These tables are supplied to each of four compressor components in the RELAP model, one representing each compressor stage (there are two, two stage compressors in the system).

The existing compressor components were reviewed, and the peripheral speed and impeller outer diameters used for the first stage low- and high-pressure compressors were found to be reversed from the design values reported in (Yan, Sato and Sumita, 2018). These values were changed to be consistent with design values.

The inlet temperature and pressure used to calculate the high-pressure compressor relative corrected flow rate and the pressure ratio were set to design conditions given in (Yan, Sato and Sumita, 2018). These values are 841.15 K for the inlet temperature and 3.67 MPa for the inlet pressure of the high-pressure compressor.

2.1.2 Heat Exchangers

The HTTR-GT/H_2 plant consists of various heat exchanger types, including helical coil, shell and tube heat exchangers, as well as an offset-strip plate and fin recuperator. While they differ in their details, the primary heat transfer configuration of these heat exchangers (except for the recuperator) is a tube bundle in crossflow. Early attempts to model one heat exchanger did not closely match the heat transfer expected from the design data using the built-in heat transfer correlations of RELAP5-3D. While RELAP5-3D includes a correlation for external flow across tube bundles, it is based on a combination of parallel and crossflow. This is appropriate for many heat exchanger designs, but the majority in this system are in a configuration closer to pure crossflow. Since RELAP5-3D allows the user to apply a surface heat flux calculated by a control variable rather than using the built-in correlations, we have implemented the "Delaware method" as described in (Serth and Lestina, 2014) via the control system for many of the heat exchanger models. The exceptions are described in their individual sections.

The Delaware method is in the form of three graphs, one for three commonly used tube bundle configurations. These graphs use the Fanning friction factor, and the Coburn j-factor given by

$$j = \frac{hPr^{2/3}}{C_P G \phi} \tag{12}$$

where h is the heat transfer coefficient, Pr is the Prandtl number, C_P is the specific heat capacity, G is the shell side mass flux, and ϕ is a viscosity correction factor (not to be confused with the flow coefficient for the turbomachinery). Approximate curve fits for the graphs are given by

$$j = a_1 \left(\frac{1.33}{P_T/D_o}\right)^a (Re)^{a_2} \tag{13}$$

$$f = b_1 \left(\frac{1.33}{P_T/D_o}\right)^b (Re)^{b_2} \tag{14}$$

where

$$a = \frac{a_3}{1 + 0.14(Re)^{a_4}} \tag{15}$$

$$b = \frac{b_3}{1 + 0.14(Re)^{b_4}} \tag{16}$$

The tube pitch is given by P_T, the tube outer diameter is D_o, and Re is the Reynolds number. The constants a_{1-4} and b_{1-4} are found in (Serth and Lestina, 2014) and are dependent on Reynolds number and orientation of the tube bank (square, triangular, or rotated square). The correlations for the heat transfer coefficient (Equations 12 and 13) can be implemented exactly with using control variables. The correlations for the friction factor cannot, but can be approximated by using the alternate turbulent wall friction model in RELAP5-3D, in which the friction factor is calculated by

$$f = A + B(Re)^{-C} \tag{16}$$

This equation has the same form as Equation 14 except for the varying dependence on pitch-to-diameter ratio. It can be seen from Equation 16 that this term approaches a constant value at high Reynolds numbers which are characteristic of the HTTR-GT/H_2 plant heat exchangers.

As part of the Delaware method various correction factors are applied to the ideal value determined with the correlations above. These correction factors are used to account for bypass flows and geometry effects. Rather than apply the geometry-based correction factors prescribed, a single factor is adjusted to best match design data. The value of this factor should be less than one, but not significantly (in the range of 0.5 to 1). A correction factor in this range will be an indication that the method is able to describe the heat exchanger in question with reasonable accuracy.

2.1.2.1 Precooler

After exiting the low-pressure turbine, the coolant enters an integrated heat exchanger that contains both the recuperator and the precooler. Heat is first recovered by the recuperator then the coolant temperature is further cooled by the precooler to reduce the compression work in the compressors. The vertically oriented precooler is a helical coil tube and shell heat exchanger with secondary helium flowing through the shell side with a diameter of 1.68 m and cooling water on the tube side. Water flows through 144 tubes (0.0288 m OD) arranged in a 9×16 bank. Radial fins are attached to the tubes to increase surface area and improve heat transfer.

The RELAP5-3D model of both the cylindrical shell and helical tubes are divided into 12 axial segments, using a pipe component for each. The tube-side heat transfer is calculating using the default (Dittus-Boelter) correlation, while the shell-side heat transfer and friction are determined using the Delaware method. The heat flux is calculated considering the effect of the fins

$$q'' = h\left[\frac{A_t}{A_{RELAP}}\left(1 - \frac{A_f}{A_t}(1 - \eta_f)\right)\right]\Delta T \tag{17}$$

Here A_f denotes the fin area, A_t the total area, A_{RELAP} the area of tubes without fins, this represents the area that RELAP5 calculates for a cylindrical heat structure. The fin efficiency is given by

$$\eta_f = \frac{(2r_1/m)}{r_{2c}^2 - r_1^2} \frac{K_1(mr_1)I_1(mr_{2c}) - I_1(mr_1)K_1(mr_{2c})}{I_0(mr_1)K_1(mr_{2c}) + K_0(mr_1)I_1(mr_{2c})} \tag{18}$$

where $r_{2c} = r_2 + t/2$, r_1 and r_2 are the inner and outer fin radii and t is the fin thickness. The fin parameter m is given in terms of the heat transfer coefficient h, fin perimeter P, thermal conductivity k, and fin cross sectional area A_c by

$$m = \sqrt{\frac{hP}{kA_c}} \tag{19}$$

The modified Bessel functions in Equation 18 are recorded in general tables in RELAP5 for a range of values of m.

To match the design heat transfer rate of 4.784 MW, the calculate heat transfer coefficient must be corrected by a value of 0.87. As mentioned previously a value less than one is expected and indicates good agreement with design values. To achieve the correct flow rates at design upstream and downstream pressures, a correction factor of 3.025 must be applied to the calculated friction factor. In this case agreement is not as close.

2.1.2.2 Cooler A

When operating in SPG mode helium exiting the high-pressure side of the recuperator is cooled in Cooler A before returning to the IHX. Cooler A is a shell-and-tube heat exchanger in which the shell-side flow makes a single pass of a U-shaped tube bank. The shell-side flow therefore approximates pure crossflow.

The secondary helium flows through the shell side of Cooler A, which has a diameter of 1.2 m. Water coolant flows through 185 tubes arranged in a U-shaped bank. Each tube has an outer diameter of 0.0254 m.

The RELAP5-3D model of Cooler A uses a pipe component to model the tube bank, divided into 22 volumes, 11 per side. The shell side of the heat transfer area is modeled using 2 volumes, one for each side of the tube bank. The heat transfer coefficient in the tubes is calculated with the default heat transfer model, and the Delaware method is used to calculate the heat transfer on the shell side.

To match the design heat transfer rate of 4.43 MW the calculated heat transfer coefficient is corrected by a factor of 0.935. This value indicates good agreement of the model and design. The friction factor, however, must be corrected by a value of 25.67 to give the correct flow rate for the design pressure drop. This value could potentially be improved with a less coarse nodalization of the shell side.

2.1.2.3 Cooler B

When operating in HCG mode helium exiting the high-pressure side of the recuperator is cooled in Cooler B before returning to the IHX. Cooler B is a shell and tube heat exchanger design in which the shell-side coolant flows back and forth through a series of baffles and therefore makes multiple passes of a U-shaped tube bank. Each coolant pass of the shell-side approximates pure crossflow.

The secondary helium coolant flow in the shell side of Cooler B, which has a diameter of 1 m. Water coolant flows through 153 tubes in a U-shaped bank. Each tube has an outer diameter of 0.0254 m.

The RELAP5-3D model of Cooler B uses a pipe component to model the tube bank, which is divided into 28 volumes (14 for each side), two between each baffle. The shell side heat transfer region is divided into 5 separate areas in which the helium passes over the tube bundle. The Delaware method is used to calculate both the heat transfer coefficient and the friction factor for the shell side. As before the default heat transfer correlation is used to calculate heat transfer in the tubes.

To match the design heat transfer rate of 4.19 MW, the heat transfer coefficient is corrected by a factor of 1.39, indicating slightly worse agreement then for the other heat transfer components. A friction tuning multiplier of 1.26 was used to achieve the correct flow rate for the design pressure drop.

2.1.2.4 Recuperator

The recuperator component is used to recover turbine exhaust heat and improve the efficiency of the system. The recuperator is an offset strip plate-fin heat exchanger consisting of 4 heat exchange modules with a total flow area of 0.154 m^2. The component has a total heat transfer area of 891 m^2 and transfers a total of 19.69 MW of heat.

The RELAP5-3D model of the recuperator was divided into 21 axial volumes for both the primary and secondary sides. The heat transfer coefficient for both sides is calculated using the default heat transfer correlation. The pressure losses in the component were chosen to obtain the pressure drop expected to match design values.

2.1.2.5 2nd IHX

When operating in HCG mode the component referred to as the 2nd IHX transfers heat from the reactor to a tertiary loop. This energy is used as process heat to improve the efficiency of the Sulfur-Iodine hydrogen generation process. The 2nd IHX is a horizontally oriented shell and helical coil tube heat exchanger. A flow guide directs the flow to flow both over and parallel to the tubes. Thus, this heat exchanger uses a combination of parallel and crossflow to transfer heat. A diagram of the 2nd IHX is shown in Figure 5.

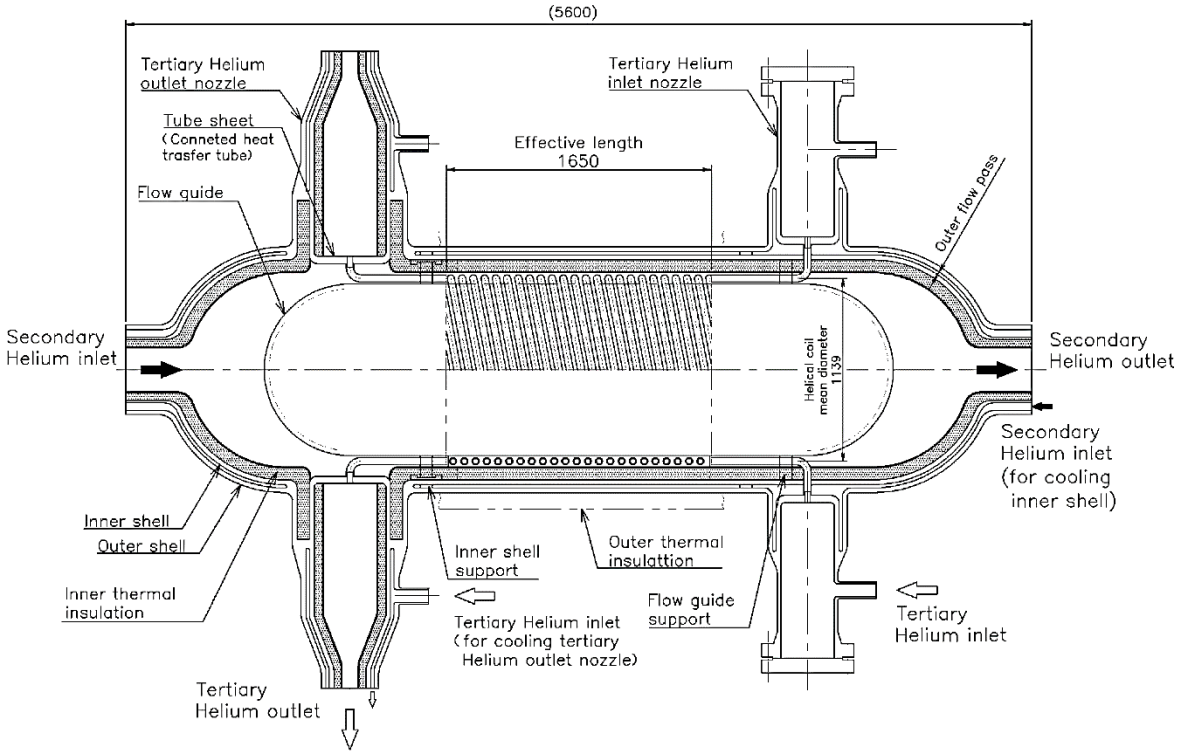

Figure 5. Diagram of the 2nd IHX component (Tanaka, 2018).

The 2nd IHX component is a shell and tube heat exchanger. The secondary helium flows through the shell side of the helical-coil 2nd IHX component with a diameter of 1.289 m. Tertiary helium flows through the tube side of the 2nd IHX with a coil diameter of 1.139 m. The tube side consists of a bank of 10 0.045 m outer diameter pipes with an effective length of 1.65 m. There is a total of 12.1 m^2 of heat transfer area between the shell and tube sides.

The RELAP5-3D model of the 2nd IHX uses a pipe component for both the shell and tubes which is divided into 12 axial segments. The tube side heat transfer is calculated using the default heat transfer correlation. The shell side heat transfer is calculated using the correlation that represents the tube bundle as a vertical bundle with crossflow, which was most appropriate for this component. The form loss coefficients were set to 0.72 to obtain an appropriate pressure drop across the component. A heat transfer multiplying factor of 2.5 was used on the turbulent forced convection heat transfer coefficient to obtain the proper heat transfer.

The model for the 2nd IHX was run independently and transferred the expected 0.7 MW of heat (Yan, Sato and Sumita, 2018) the other results were representative of design conditions.

2.1.2.6 IHX

The IHX component model that transfers heat from the primary system to the secondary system was provided by JAEA. After inspecting the RELAP5 model the surface roughness was reduced and the friction was increased by a factor of 2.2 to better match design values for temperature and pressure drop.

The two specific operation modes required some additional changes. These changes are described in the following sections.

3.1 Changes for HCG mode

3.1.1 Flow splitting for cogeneration mode

A servo valve was added to the model so that the heated helium gas was appropriately split for electricity and hydrogen cogeneration. In HCG mode a portion of the reactor heat is used for electricity generation and the remainder for hydrogen generation via the sulfur-iodine process.

The servo valve was added to the RELAP5 model to control the helium mass flow rate of 6.58 kg/s for the coolant traveling through the green loop shown in Figure 1 between Cooler B and the 2nd IHX. The mass flow rate through the servo valve was set with a control variable.

3.1.2 Boundary conditions modifications for HCG mode

Various boundary conditions were changed for the cogeneration model. The inlet temperature of the tertiary helium loop of the 2nd IHX was reduced from a value of 766.15 K to 623.15 K per design conditions (Imai, Sato, et al., 2017).

The boundary conditions for the reactor primary system are different depending on the operation mode. The reactor primary outlet temperature and the mass flow rate were modified to match design conditions. The reactor outlet temperature for the HCG mode is changed from 1123.15 to 1223.15 K and the mass flow rate through the primary system is reduced from 4.16 to 3.47 kg/s (Imai, Sato, et al., 2017).

4.1 Transient Analysis

When the secondary system operation is switched from SPG to HCG mode the mass flow rate through the IHX that transfers heat between the primary and secondary systems is reduced. The cooling capability of the IHX is decreased with the change in mass flow rate, which results in an increase in the primary system coolant temperature. The potential reactivity response due to the primary coolant temperature increase is evaluated.

In an actual transient scenario both the reactor inlet and outlet temperatures would change based on a reduced heat load. However, the reactor itself is not a part of this model and the core outlet temperature is set to a constant value. The increase in the reactor outlet temperature due to the reduced heat load is not reflected in the transient. The temperature of the primary system coolant exiting the IHX will increase, and it is assumed that the amount of temperature increase is reflected in the reactor in entirety. No other reactivity changes are considered in this analysis.

The zero-power isothermal temperature coefficients for the HTTR are reported in (Bess and Fujimoto, 2014). These reported values were plotted, and a curve-fit was developed to correlate the reactivity and temperature. The plotted zero-power isothermal temperature coefficients and the linear fit generated in Excel are shown in Figure 6.

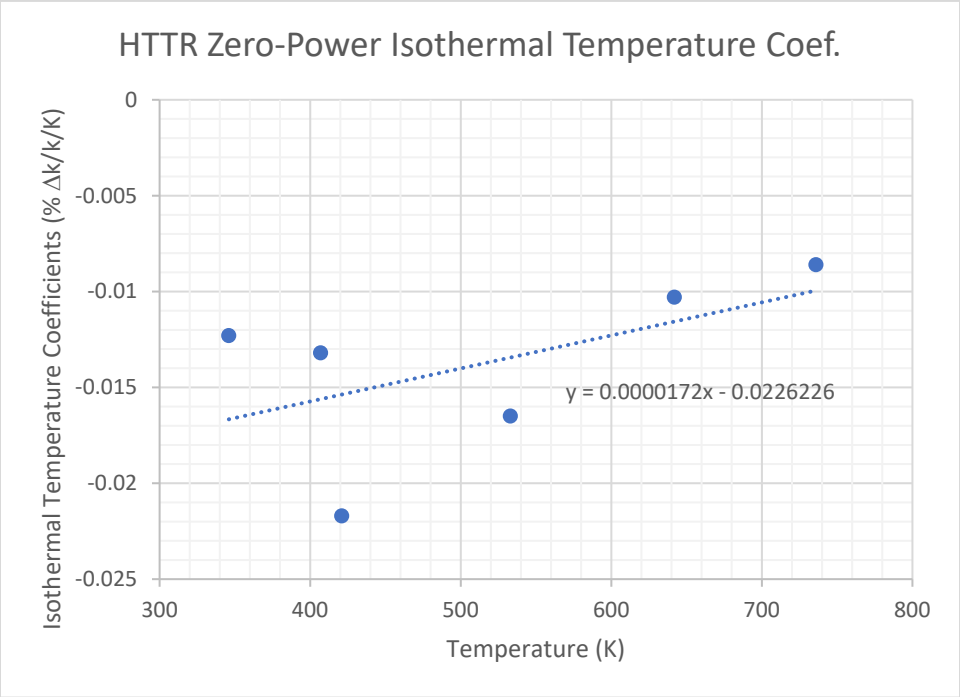

Figure 6. HTTR zero-power isothermal temperature coefficients as a function of temperature.

5.1 Results

5.1.1 Steady-State

The revised input decks were run for both the sole power and helium cogeneration modes. When the SPG case was first run, the calculated mass flow rates were lower than the design values. The largest pressure drop was observed across the turbine components, so the loss factors across the turbines were reduced slightly to improve mass flow rate results. After this change the mass flow rates were in excellent agreement with design conditions.

The results for the SPG mode are shown in Table 1. The largest difference in temperature results were within about 7 K. The pressures were also in good agreement, with the largest differences on the order of 0.05 MPa. RELAP5-3D underpredicts the pressure at certain points, but the magnitude of the differences was small.

Table 1. RELAP5-3D predictions of the HTTR-GT/H_2 secondary system state points for sole-power generation mode compared to design values.

Location	Temperature [K]		ΔT [K]		Pressure [MPa]		ΔP [MPa]	
	Design	RELAP	Design	RELAP	Design	RELAP	Design	RELAP

IHX secondary side outlet	843.15	846.06	-	-	4.11	4.103	-	-
Turbine inlet	841.35	842.68			4.059	4.059		
Turbine outlet	776.65	782.09	-64.7	-60.59	3.152	3.101	-0.907	-0.958
Recuperator LP side inlet	776.65	782.09			3.151	3.100		
Recuperator LP side outlet	391.65	394.22	-385	-387.87	3.143	3.092	-0.008	-0.009
Precooler inlet	391.65	394.22			3.143	3.092		
Precooler outlet	298.15	298.17	-93.5	-96.05	3.14	3.088	-0.003	-0.004
Compressor inlet	298.15	298.17			3.13	3.087		
Compressor outlet	348.85	353.87	50.7	55.7	4.307	4.307	1.177	1.220
Recuperator HP side inlet	348.85	353.85			4.304	4.306		
Recuperator HP side outlet	733.85	740.76	385	386.91	4.298	4.300	-0.006	-0.007
Cooler A inlet	733.85	740.7			-	4.297		
Cooler A outlet	647.15	652.05	-86.7	-88.65	-	4.267	-	-0.030
IHX secondary side inlet	647.15	652.14			4.26	4.264		

The results for the HCG mode are shown in Table 2. The mass flow rates are not reported but fit the case well. The temperature and pressure results did not match design values as well for the HCG case. The largest differences were observed across the turbine component. The largest temperature differences reported by RELAP5-3D occurred at the turbine outlet and near the inlet to Cooler B. These differences were approximately 35-39 K.

The pressure differences were also larger for the HCG mode. The largest pressure drop occurs across the turbine components which could be due to RELAP5-3D calculating a loss factor that is too large. The pressure drop across the turbine is approximately 0.17 MPa. The largest pressure difference (about 0.27 MPa) is observed at the compressor outlet.

The compressor component did not increase the pressure of the system as significantly as expected, the implementation of the pressure ratio for this component may need some refinement. The recuperator was also observed to transfer less heat than expected. There may be a need to increase the heat exchange area of this component to improve the results.

The differences in temperature and pressure are primarily attributed to the complexity of the various components and the flow split for the HCG mode in the secondary loop. The largest differences appear in locations where the coolant flow is either split or combined.

Table 2. RELAP5-3D predictions of the HTTR-GT/H_2 secondary system state points for hydrogen cogeneration mode compared to design values.

Location	Temperature [K]		ΔT [K]		Pressure [MPa]		ΔP [MPa]	
	Design	RELAP	Design	RELAP	Design	RELAP	Design	RELAP
IHX secondary side outlet	1173.15	1172.8	-	-	4.11	4.1093	-	-
2nd IHX secondary side inlet	1160.55	1170.5			-	4.10317		
2nd IHX secondary side outlet	1108.15	1116.3	-52.4	-54.2	-	4.09988	-	-0.00329
Turbine inlet	841.35	815.13			4.077	4.07664		
Turbine outlet	779.45	740.13	-61.9	-75	3.283	3.11917	-0.794	-0.95747

Recuperator LP side inlet	779.45	740.13			3.282	3.11874		
Recuperator LP side outlet	389.65	379.23	-389.8	-360.9	3.275	3.11257	-0.007	-0.00617
Precooler inlet	389.65	379.23			3.267	3.11248		
Precooler outlet	298.15	297.22	-91.5	-82.01	3.265	3.10906	-0.002	-0.00342
Compressor inlet	298.15	297.23			3.265	3.10865		
Compressor outlet	347.35	341.76	49.2	44.53	4.402	4.13551	1.137	1.02686
Recuperator HP side inlet	347.35	341.75			4.138	4.13448		
Recuperator HP side outlet	737.15	702.02	389.8	360.27	4.134	4.13032	-0.004	-0.00416
Cooler B inlet	737.15	702.06			-	4.13019		
Cooler B outlet	423.15	420.42	-314	-281.64	-	4.12857		-0.00162
IHX secondary side inlet	423.15	422.57			4.125	4.12832		

5.1.2 Transient

The transient was performed by reducing the rotational speed of the compressors by approximately 5%. The scenario was run for 2500 s until the primary system temperature stabilized. The secondary system mass flow rate is reduced and nearly levels off at 7.25 kg/s around 1600 s into the transient as shown in Figure 7.

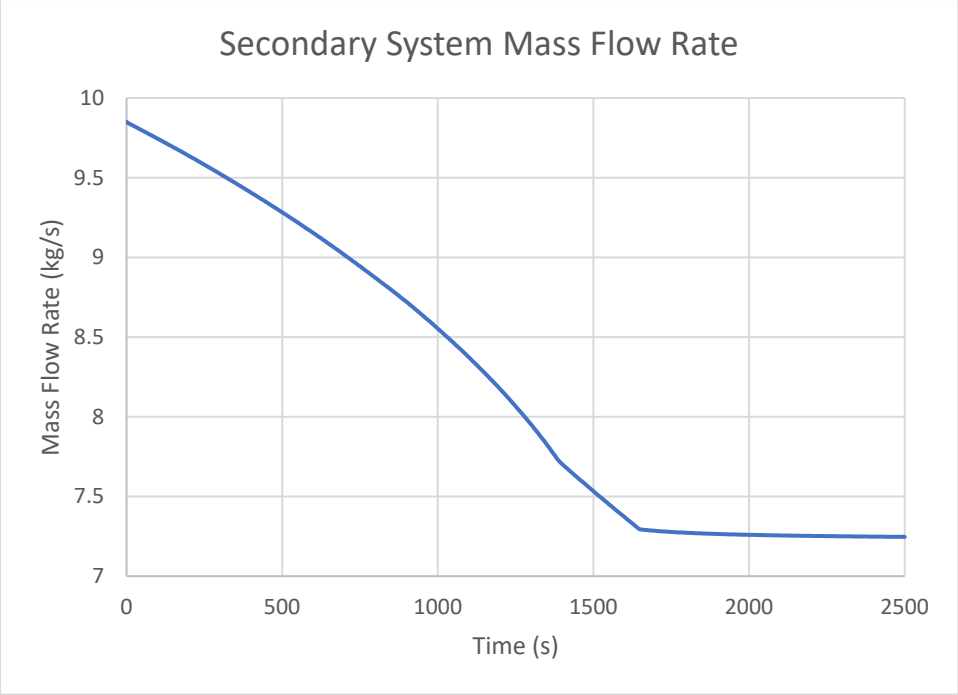

Figure 7. Secondary system mass flow rate.

The average coolant temperature in the core is calculated by taking the average of the core inlet and outlet temperatures and adding the temperature rise due to the reduced heat transfer in the IHX. The core average temperature and the associated temperature reactivity response are shown in Figure 8. The reactivity added to the core due to the temperature rise is expected to remain negative throughout the transient. This reactivity addition is a passive safety feature of the reactor.

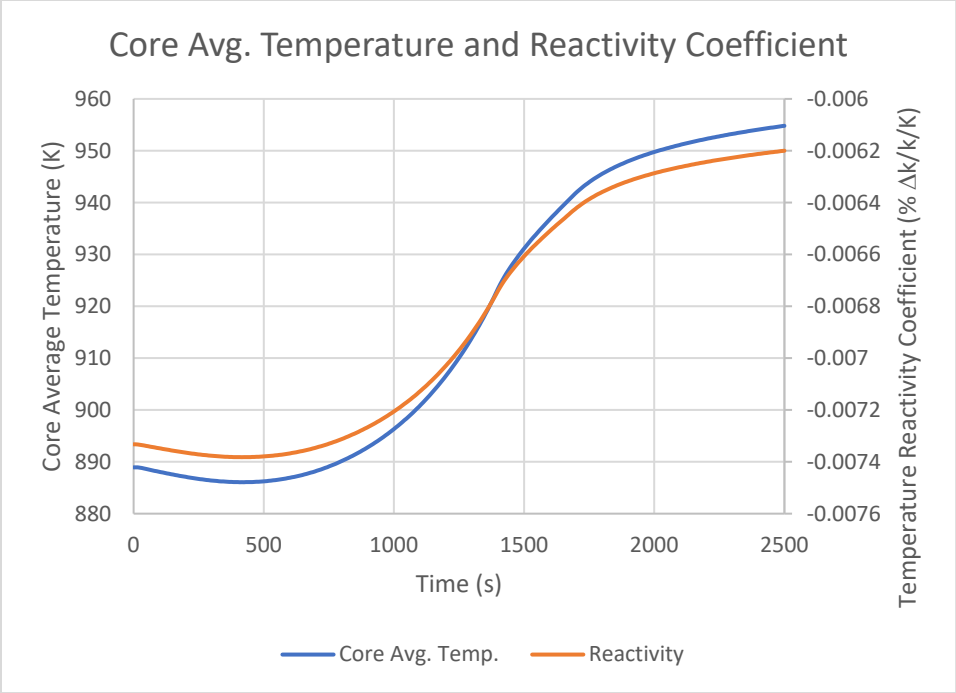

Figure 8. Core average temperature and temperature reactivity coefficient during the transient.

6.1 Conclusions

The HTTR-GT/H_2 test plant is being designed to use a high-temperature gas reactor to generate both electricity and hydrogen based on demand. RELAP5-3D models were developed for both the sole-power and hydrogen cogeneration modes. These models were executed, and results were compared to design conditions. It was found that the results for the sole-power generation mode compared very favorably to design conditions. The largest temperature and pressure deviations from design conditions are about 7 K and 0.05 MPa, respectively.

Larger differences were observed for the hydrogen cogeneration mode. The largest temperature and pressure deviations from design conditions are about 39 K and about 0.27 MPa, respectively. The larger differences for the HCG mode are primarily attributed to the complexity of the various components and the flow being split in the secondary loop.

The pressure ratio of the compressor component and the heat exchange area of the recuperator are two areas that could potentially improve the calculation.

A transient scenario was investigated in which the heat removal capability of the secondary system was reduced. The core reactivity response calculation showed that a resulting temperature increase will add negative reactivity to the reactor. This negative reactivity is a passive safety feature. Future calculations may include a linked primary and secondary system to demonstrate potential affects off normal conditions in the secondary system may have on the primary system.

7.1 References

Pioro, I., Duffey, R., "Current and Future Nuclear Power Reactors and Plants", Managing Global Warming, 2019, pp. 117-197.

IAEA, "High Temperature Gas Cooled Reactor Fuels and Materials", IAEA-TECDOC-1645, Vienna, 2010.

HTTR Website, https://httr.jaea.go.jp/eng/index.html, accessed 9/14/20.

Fujikawa, S., Hayashi, H., et al., "Achievement of Reactor Outlet Coolant Temperature of 950°C in HTTR", Journal of Nuclear Science and Technology, Vol. 41, Issue 12, June 2004, pp, 1245-1254.

The RELAP5-3D© Code Development Team, "RELAP5-3D© Code Manual Volume I: Code Structure, System Models and Solution Methods", INL/MIS-15-36723, Rev. 4.4, June 2018.

Sterbentz, J. W., Bayless, P. D., "High Temperature Gas-Cooled Test Reactor Options Status Report", INL/EXT-15-36340, Aug. 2015.

Davis, C., Siefken, L. J., et al., "Assessment of RELAP5-3D for Analysis of Very High Temperature Gas-Cooled Reactors", INL/CON-05-00282, NURETH-11, Oct. 2005.

Humrickhouse, P. W., "RELAP5-3D Model of the HTTR-GT/H_2 Secondary System and Turbomachinery", INL/LTD-18-45714, August 2018.

Sato, H., Nomoto, Y., et al., "HTTR-GT/H_2 Test Plant - System Performance Evaluation for HTTR Gas Turbine Cogeneration Plant", p. 759-766, Proc. HTR 2016, Las Vegas, NV, November 6-10, 2016.

Yan, X. L., Sato, H., et al., "HTTR-GT/H_2 Test Plant – System Design", p. 827-836, Proc. HTR 2016, Las Vegas, NV, November 6-10, 2016.

Tsukamoto H., Oyama, S., et al., "HTTR-GT/H_2 Test Plant – Design Study on Helium Gas Turbine for the Heat Utilization System Connected to JAEA's HTTR", p. 837-844, Proc. HTR 2016, Las Vegas, NV, November 6-10, 2016.

Tanaka K., et al., HTTR-GT/H_2 test plant - conceptual design study on new intermediate heat exchanger, p. 419-425, Proc. HTR 2016, Las Vegas, NV, November 6-10, 2016.

Imai, Y., Sato, H., Yan, X. L., "Design Database of Helium Gas Turbine for High Temperature Gas-cooled Reactor", Information based on JAEA-Data/Code 2017-011, Rev. 1, JAEA, August 25, 2017.

Yan, X. L., Sato, H., Sumita, J., et al., "Design of HTTR-GT/H_2 Test Plant", Nuclear Engineering and Design 329, 2018, pp. 223-233.

Serth, R. W., Lestina, T. G., "Process Heat Transfer: Principles, Applications, and Rules of Thumb", Second Edition, Ch. 6, Academic Press, Oxford, 2014.

Bess, J. D., Fujimoto, N., "Benchmark Evaluation of Start-Up and Zero-Power Measurements at the High-Temperature Engineering Test Reactor", Nuclear Science and Engineering 178, 2014, pp. 414-427.